Inorganica Chimica Acta, 133 (1987) 81–91

Binuclear Copper(II) Complexes of some Tetradentate (N_4) Diazine Ligands with Benzimidazole Donor Groups. Crystal Structure of [μ-3,6-Bis(*N*-ethyl-2-benzimidazolylthio)pyridazine-*N*, μ-N^5, μ-N^6, *N*]-(μ-hydroxo)(μ-chloro)dichlorodicopper(II) DMF*

LAURENCE K. THOMPSON,** SANAT K. MANDAL, LISA ROSENBERG

Department of Chemistry, Memorial University of Newfoundland, St. John's, Nfld., A1B 3X7, Canada

FLORENCE L. LEE and ERIC J. GABE

Division of Chemistry, National Research Council, Ottawa, Ont., K1A 0R6, Canada

(Received January 21, 1987)

Abstract

Binuclear copper(II) and copper(I) complexes and mononuclear copper(II) complexes of a series of *N*-alkyl substituted derivatives of the tetradentate ligand 3,6-bis(2-benzimidazolylthio)pyridazine (BITP) are reported. The complex $[Cu_2(EtBITP)(OH)Cl_3]\cdot DMF$ **(II)** contains a triply bridged binuclear centre with a diazine (N–N), a hydroxide and a chloride bridge. The two trigonal-bipyramidal copper(II) centres are separated by 3.017 Å with a Cu–O(H)–Cu bridge angle of 104.7° and are antiferromagnetically coupled ($-2J = 260$ cm^{-1}). Cyclic voltammetric studies on several binuclear copper(II) complexes show quasi-reversible or essentially non-reversible redox waves at positive potentials (0.41–0.46 V *versus* SCE) associated with two electron reduction.

Complex **II** forms green crystals with $a = 8.9198(5)$, $b = 13.5738(8)$, $c = 13.7178(7)$ Å, $\alpha = 105.318(5)°$, $\beta = 105.255(5)°$, $\gamma = 99.461(5)°$, $P\bar{1}$, $Z = 2$, $R_f = 0.028$.

Introduction

Binucleating, tetradentate (N_4), diazine ligands involving pyridazine produce predominantly hydroxo-bridged dicopper(II) complexes in which the copper(II) centres are antiferromagnetically coupled [1–8] (Fig. 1). Although variable temperature magnetic studies do not appear to have been carried out on hydroxo-bridged complexes of DPPN [5–8], the large hydroxide bridge angles (122–128°) observed for these $d_{x^2-y^2}$ ground state systems would suggest the presence of very strong antiferromagnetic exchange between the copper(II) centres [9–12].

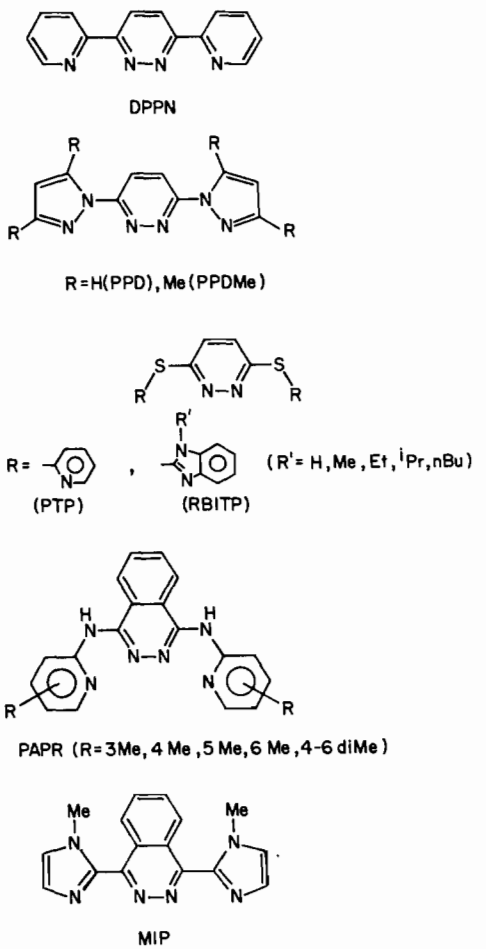

Fig. 1. Binucleating pyridazine and phthalazine ligands.

Binuclear hydroxo-bridged copper(II) complexes of the related pyrazolylpyridazine ligands PPD, PPDMe (Fig. 1) have generally smaller hydroxide bridge angles (116–120°) [2, 3] but exhibit very strong

*This paper assigned NRCC Contribution No. 27821.

**Author to whom correspondence should be addressed.

0020-1693/87/$3.50

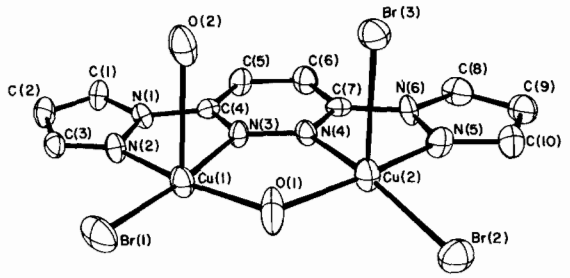

Fig. 2. Structural representation of $[Cu_2(PPD)(OH)Br_3(H_2O)]\cdot 0.6H_2O$ with hydrogen atoms and water omitted (40% ellipsoids).

antiferromagnetic exchange between the square-pyramidal copper(II) centres ($[Cu_2(PPD)(OH)Cl_3(H_2O)]\cdot 0.8H_2O$, $-2J = 898 \pm 13$ cm^{-1}; $[Cu_2(PPD)(OH)Br_3(H_2O)]\cdot 0.6H_2O$ (Fig. 2), $-2J = 1304 \pm 72$ cm^{-1}; $[Cu_2(PPDMe)(OH)(NO_3)_2(H_2O)_2]NO_3\cdot H_2O$, $-2J = 770 \pm 3$ cm^{-1} [3, 13]). The five-membered chelate rings generated by this class of ligands, including the pyridylpyridazine DPPN, of necessity create larger hydroxide bridge angles than those observed with pyridylaminophthalazine ligands (PAPR, Fig. 1) involving six-membered chelate rings (Cu–O(H)–Cu = 100–116°) [9, 11, 12] and as a consequence antiferromagnetic coupling between the copper(II) centres is smaller ($-2J < 600$ cm^{-1}) for these systems. The ligand PTP (Fig. 1), which involves an exocyclic sulfur bridge between the peripheral pyridine and the pyridazine moiety, has been shown to form a binuclear copper(II) derivative involving two chloro-bridges ($-2J = 131$ cm^{-1}) [14] and also hydroxo-bridged derivatives [4].

In the present study we have examined the copper coordination chemistry of a series of related sulfur bridged ligands (RBITP, Fig. 1) involving *N*-alkyl substituted benzimidazole groups. Both binuclear copper(II) and copper(I) derivatives have been produced and in all cases so far studied the binuclear copper(II) complexes appear to be hydroxo-bridged. An X-ray study on the complex $[Cu_2(EtBITP)(OH)Cl_3]\cdot DMF$ (**II**) reveals a triply bridged binuclear structure involving hydroxo- and chloro-bridges in addition to the diazine bridge. The five-coordinate copper(II) centres have stereochemistries that can best be described as distorted trigonal-bipyramidal. This feature distinguishes this system from other analogous five-coordinate derivatives where the five-coordination most closely approached that of a square-pyramid. A variable temperature magnetic study on **II** indicates modest antiferromagnetic exchange between the copper(II) centres ($-2J = 260$ cm^{-1}).

Experimental

Magnetic susceptibilities were obtained at room temperature by the Faraday Method using a Cahn Model 7600 Faraday Magnetic Susceptibility System coupled to a Cahn gram electrobalance. Variable temperature magnetic susceptibility data were obtained (compound **II**) in the range 5–300 K using an Oxford Instruments Superconducting Faraday Susceptometer with a Sartorius 4432 microbalance. A main solenoid field of 1.5 Tesla and a gradient field of 10 Tm^{-1} were employed.

The electrochemical measurements were performed at room temperature in dimethylformamide (DMF) (spectroscopic grade dried over molecular sieves) under O_2-free conditions using a BAS CV27 Voltammograph and a Houston Omnigraph 2000 X-Y recorder. A three electrode system was used (cyclic voltammetry) in which the working electrode was either glassy carbon or platinum, the counter electrode platinum, with a standard calomel (SCE) electrode as reference. For coulometry measurements a three electrode system was employed consisting of a platinum mesh flag working electrode, a platinum mesh counter electrode and a silver rod as reference electrode. The supporting electrolyte was tetraethylammonium perchlorate (TEAP) (0.1 M) and all solutions were 10^{-3}–10^{-4} in complex. Infrared spectra were obtained with a Perkin-Elmer 283 and UV–Vis spectra with a Cary 17. NMR spectra were run as solutions in $CDCl_3$ using a Bruker WP80 spectrometer ($SiMe_4$ internal standard) and mass spectra were obtained using a V.G. Micromass 7070 HS spectrometer with a direct insertion probe. C, H and N analyses were carried out by Canadian Microanalytical Service, Vancouver. Copper analyses were determined by atomic absorption with a Varian Techtron AA-5, after digestion of the samples in concentrated HNO_3.

Synthesis of Ligands and Copper Complexes

3,6-bis(N-isopropyl-2-benzimidazolylthio)-pyridazine (iPrBITP)

BITP [4] (7.5 g, 20 mmol), K_2CO_3 (14 g, 0.10 mol), isopropylbromide (7.4 g, 60 mmol) and acetonitrile (120 ml) were refluxed together with stirring for 24 h. The brownish slurry was filtered hot and the precipitate washed with hot acetonitrile (50 ml) and the filtrate cooled in ice. A cream coloured product formed which was filtered, washed with petroleum ether and dried under vacuum. More product was obtained on reducing the volume of the filtrate (yield 35%, melting point (m.p.) 185–189 °C). *Anal.* Calc. for $C_{24}H_{24}N_6S_2$: C, 62.6; H, 5.22; N, 18.3. Found: C, 62.5; H, 5.20; N, 18.5%.

The other ligands, involving methyl (yield 15%, m.p. 217–222 °C), ethyl (yield 30%, m.p. 204–207 °C) and n-butyl (yield 45%, m.p. 186–189 °C) substituents were prepared in a similar manner. Satisfactory elemental analyses were obtained for all compounds. The following NMR and mass spectral

data were obtained for the ligands. Mass spectrum, major mass peaks (*m/e* (relative intensity)); MeBITP 404(13) P, 241(29), 161(100), 144(9), 131(21), 129-(14), 119(30). Et(BITP) 432(4) P, 255(100), 227-(13), 177(24), 150(16), 144(5), 119(9). iPrBITP 460(4) P, 269(100), 227(58), 192(40), 150(63), 119(10). BuBITP 488(9) P, 431(3), 283(100), 253-(4), 227(44), 205(35), 173(35), 150(25), 119(20), 90(9). Nuclear magnetic resonance data (ppm); MeBITP($CDCl_3$) 7.72(m, 4H), 7.32(s, 2H), 7.28(m, 4H), 3.72(s, 6H). EtBITP($CDCl_3$) 7.70(m, 4H), 7.35-(s, 2H), 7.27(m, 4H), 4.33(q, 4H), 1.37(t, 6H). iPrBITP($CDCl_3$) 7.63(m, 4H), 7.29(s, 2H), 7.20(m, 4H), 5.1(m, 2H), 1.57(d, 12H). BuBITP($CDCl_3$) 7.68-(m, 4H), 7.35(s, 2H), 7.25(m, 4H), 4.25(m, 4H), 1.75(m, 4H), 1.28(m, 4H), 0.9(m, 6H). Each ligand is characterized by exhibiting two low field multiplets associated with the alpha and beta benzimidazole, aromatic protons, a single resonance associated with the pyridazine protons and typical aliphatic proton resonances at higher fields.

[Cu_2(EtBITP)(OH)Cl_3]·DMF (II)

EtBITP (0.5 g, 1.2 mmol) was dissolved with warming in DMF (50 ml) and mixed with a solution of $CuCl_2 \cdot 2H_2O$ (0.50 g, 2.9 mmol) in water (10 ml). The resulting green solution was warmed and allowed to stand for several days during which time green crystals deposited. The product was filtered, washed with ethanol and finally with ether and dried *in vacuo*. Compound **III** was prepared in a similar manner.

Compounds **I**, **IV**, **VI**, **VII**, **IX**, **X**, **XI** were prepared similarly by dissolving the metal salt in water and the ligand in methanol.

[Cu(BuBITP)]$_2$(ClO_4)$_2$·0.2H_2O (XII)

BuBITP (0.50 g; 1.0 mmol) was dissolved in degassed dichloromethane (50 ml). [$Cu(CH_3CN)_4$]-ClO_4 (0.33 g; 2.0 mmol) was added under nitrogen and the mixture stirred for 20 min at room temperature. The orange solution was filtered to remove excess cuprous perchlorate and degassed methanol (50 ml) added to the filtrate. An orange crystalline solid formed which was filtered, washed with methanol and petroleum ether and dried *in vacuo*. Complexes **V** and **VIII** were prepared similarly.

Analytical data for the copper complexes are given in Table 1.

Crystallographic Data Collection and Refinement of the Structure of [Cu_2(EtBITP)(OH)Cl_3]·DMF (II)

Crystals of **II** are green in colour. The diffraction intensities of an approximately 0.30 × 0.15 × 0.12 mm crystal were collected with graphite monochromatized Mo Kα radiation using the omega scan technique to $2\theta_{max} = 45°$ on a Nonius CAD4 diffractometer. Of a total of 4193 measured reflections

TABLE I. Analytical and Other Data

	Compound	Colour	Found (%)				Calc. (%)			
			C	H	N	M	C	H	N	M
I	[Cu_2(MeBITP)(OH)Cl_3]·H_2O	dark green	35.8	2.66	12.6	19.0	35.7	2.83	12.5	18.9
II	[Cu_2(EtBITP)(OH)Cl_3]·DMF	green	39.8	3.73	13.0		39.7	3.71	13.0	
III	[Cu_2(EtBITP)(OH)Br_3]·DMF	green	33.9	3.19	11.0	14.0	33.8	3.04	11.0	14.3
IV	[Cu(EtBITP)(NO_3)$_2$]·H_2O	dark green	41.6	3.36	17.6	9.36	41.4	3.45	17.6	9.96
V	[Cu(EtBITP)]$_2$(ClO_4)$_2$·4H_2O	red–brown	42.0	3.29	13.3		41.8	3.80	13.3	
VI	[Cu_2(iPrBITP)(OH)Cl_3]·0.5H_2O	bright green	39.8	3.44	11.6	17.0	40.0	3.61	11.7	17.6
VII	[Cu_2(iPrBITP)(OH)Br_3]·0.5H_2O	green	33.8	2.99	9.86	14.0	33.8	3.05	9.85	14.9
VIII	[Cu(iPrBITP)]$_2$(ClO_4)$_2$·CH_3CN·2H_2O	red	45.0	3.78	13.6		45.1	4.14	13.7	
IX	[Cu_2(BuBITP)(OH)Br_3]	lime green	35.7	3.39	9.62	14.5	35.8	3.33	9.64	14.6
X	[Cu(BuBITP)(NO_3)$_2$]·1.5H_2O	turquoise	44.4	4.05	16.0		44.4	4.41	15.9	
XI	[Cu(BuBITP)$_2$(H_2O)](ClO_4)$_2$·3H_2O	turquoise	47.6	4.52	12.9	4.87	47.6	4.88	12.8	4.85
XII	[Cu(BuBITP)]$_2$(ClO_4)$_2$·0.2H_2O	orange	47.7	4.29	12.8	8.97	47.8	4.32	12.9	9.73

4116 were unique and 3410 were considered significant with $I_{net} > 2.5\sigma(I_{net})$. Lorentz and polarization factors were applied but no correction was made for absorption. The cell parameters were obtained by the least-squares refinement of the setting angles of 78 reflections with 2θ in the range 40°–45° (λ(Mo $K\alpha_1$) = 0.70930 Å).

The structure was solved by direct methods using MULTAN [15] and refined by full matrix least-squares methods to final residuals of $R_f = 0.028$ and $R_w = 0.018$ for the significant data (0.037 and 0.018 for all data) with weights based on counting statistics. The hydrogen atoms were located from difference maps with the positional parameters refined and the thermal parameters fixed at the calculated value. All calculations were performed with the NRCVAX system of programs [16] and scattering factors were taken from ref. 17. Crystal data are given in Table I and final atomic positional parameters and equivalent isotropic temperature factors are listed in Table II. See also 'Supplementary Material'.

TABLE II. Crystal Data

Compound	$[Cu_2(EtBITP)(OH)Cl_3]\cdot DMF$
Formula	$C_{25}H_{28}N_7O_2S_2Cl_3Cu_2$
Formula weight	755.85
Crystal system	triclinic
Space group	$P\bar{1}$
a (Å)	8.9198(5)
b (Å)	13.5738(8)
c (Å)	13.7178(7)
α (°)	105.318(5)
β (°)	105.255(5)
γ (°)	99.461(5)
V (Å^3)	1495.83
Z	2
ρ(calc) (g cm^{-3})	1.679
Crystal size (mm)	0.30 × 0.15 × 0.12
Crystal colour	green
Radiation (Å)	Mo $K\alpha_1$ (0.70930)
μ (mm^{-1})	1.87
2θ scan range (°)	45
Data collected	4193
Unique data	4116
With $I > 2.5\sigma(I)$	3410
L.S. parameters	455
Data parameters	69
R_f (significant data)	0.028
R_w (significant data)	0.018
Temperature for data collection (°C)	22
Diffractometer	Nonius

Results and Discussion

Diazine ligands, in particular pyridazines and phthalazines, are capable of binding two metal centres in close proximity by virtue of the juxtaposition of the two adjacent nitrogen donor centres in the diazine ring. Metal–metal separations have been observed in the range 3.00–3.21 Å for binuclear, hydroxo-bridged, copper(II) complexes of a series of pyridylaminophthalazine ligands (PAPR, Fig. 1) which form six-membered chelate rings [2, 9, 10–12] and in the range 3.34–3.45 Å for binuclear, hydroxo-bridged, copper(II) complexes of tetradentate pyridazine and phthalazine ligands (DPPN, PPD, PPDME, MIP; Fig. 1), which form five-membered chelate rings [1–3, 5–8, 10]. The distinct difference in copper–copper separations generated by these two groups of ligands can be attributed to the geometrical requirements of the various chelate rings at the binuclear centre (Fig. 3). Ligands like MIP, involving five-membered chelate rings, would, of necessity, generate expanded binuclear centres. These trends in binuclear centre dimensions are reflected also in the magnitude of the hydroxide bridge angle.

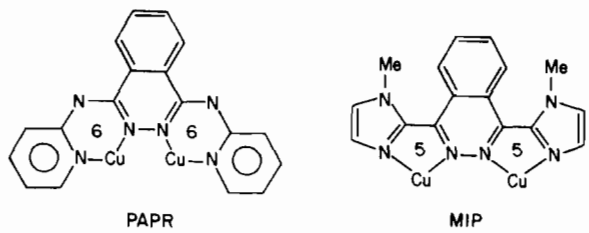

Fig. 3. Comparison of binuclear centres of diazine ligands forming six- and five-membered chelate rings.

Almost all of the complexes involving hydroxide bridges, so far characterized structurally, have five-coordinate copper(II) centres for which the most appropriate structural description would be square-pyramidal. The complex $[Cu_2(EtBITP)(OH)Cl_3]\cdot$DMF has a binuclear hydroxo-bridged copper(II) structure involving distorted five-coordinate copper(II) centres but for the first time the copper stereochemistry approximates a trigonal-bipyramid more closely than a square-pyramid.

Description of the Structure

The structure of $[Cu_2(EtBITP)(OH)Cl_3]\cdot$DMF (**II**) is shown in Fig. 4. Final atomic positional parameters are given in Table III and selected bond lengths and bond angles in Table IV. The two copper(II) centres are bound in a triple bridged arrangement involving a chloro-bridge, a hydroxo-bridge and a pyridazine diazine bridge. The angle at the hydroxo-bridge is 104.65° while that at chlorine is 72.50° with a copper–copper separation of 3.017 Å. The bridging copper–chlorine bonds are fairly long (Cu(1)–Cl(3) 2.564 Å; Cu(2)–Cl(3) 2.538 Å) while the terminal copper–chlorine bonds are much shorter (Cu(1)–Cl(1) 2.258 Å; Cu(2)–Cl(2) 2.261 Å). A comparable situation was observed for the complex $[Cu_2$-

TABLE III. Atomic Positional Parameters (e.s.d.s) for $[Cu_2(EtBITP)(OH)Cl_3]\cdot DMF$ (II)

Atom	*x*	*y*	*z*	B_{iso}
Cu1	0.28039(5)	0.78229(3)	0.95991(3)	2.484(26)
Cu2	0.14836(5)	0.91304(3)	0.82744(3)	2.534(25)
Cl1	0.31559(12)	0.78681(7)	1.13033(7)	3.54(6)
Cl2	0.03068(11)	1.04736(7)	0.86516(8)	3.30(6)
Cl3	0.02488(11)	0.72078(7)	0.79746(7)	3.24(5)
S1	0.65618(11)	0.74098(7)	0.95817(8)	3.08(5)
S2	0.38460(11)	1.00958(8)	0.69022(8)	3.32(6)
O1	0.2309(3)	0.91505(19)	0.97160(19)	2.68(14)
O2	0.3628(5)	0.70411(28)	0.61122(30)	9.50(28)
N1	0.3411(3)	0.64752(20)	0.92185(20)	2.04(16)
N2	0.0895(3)	0.89538(21)	0.67324(21)	2.30(17)
N3	0.4913(3)	0.53564(21)	0.88678(21)	2.10(16)
N4	0.1172(3)	0.90944(21)	0.51961(23)	2.37(16)
N5	0.4379(3)	0.83640(19)	0.87900(20)	2.01(16)
N6	0.3784(3)	0.89529(20)	0.82018(20)	1.95(15)
N7	0.2309(4)	0.53482(30)	0.57261(28)	4.24(23)
C1	0.2473(4)	0.54493(26)	0.89337(25)	2.00(19)
C2	0.0904(4)	0.50944(30)	0.88924(29)	2.65(22)
C3	0.0325(5)	0.40253(32)	0.86442(31)	3.18(23)
C4	0.1284(5)	0.33332(29)	0.84527(31)	3.21(24)
C5	0.2838(5)	0.36635(28)	0.84740(28)	2.65(23)
C6	0.3421(4)	0.47490(26)	0.87289(25)	2.05(20)
C7	0.4839(4)	0.63802(26)	0.91721(26)	2.06(19)
C8	0.5825(4)	0.82229(24)	0.88546(25)	1.94(18)
C9	0.6843(4)	0.87406(28)	0.84344(29)	2.24(19)
C10	0.6250(4)	0.93322(27)	0.78477(28)	2.23(20)
C11	0.4668(4)	0.93801(24)	0.77160(25)	1.99(19)
C12	0.1887(4)	0.92957(26)	0.62602(28)	2.38(20)
C13	−0.0419(4)	0.85881(26)	0.49728(29)	2.29(21)
C14	−0.1720(5)	0.82556(29)	0.40386(29)	2.88(23)
C15	−0.3184(5)	0.78319(31)	0.41093(33)	3.36(23)
C16	−0.3344(5)	0.77128(30)	0.50526(35)	3.22(24)
C17	−0.2054(5)	0.80252(30)	0.59716(31)	2.80(22)
C18	−0.0582(4)	0.84862(26)	0.59273(28)	2.24(20)
C19	0.6255(5)	0.49581(30)	0.86439(32)	2.86(23)
C20	0.6281(6)	0.48948(40)	0.75349(39)	4.32(30)
C21	0.1934(5)	0.92240(33)	0.44040(33)	3.38(25)
C22	0.2506(6)	0.82774(44)	0.39690(42)	5.39(35)
C23	0.2797(6)	0.63678(46)	0.63089(39)	5.99(35)
C24	0.1345(6)	0.45726(45)	0.60101(43)	5.72(35)
C25	0.2744(8)	0.49806(47)	0.47811(49)	6.96(44)
HO	0.167(4)	0.9179(28)	0.9993(29)	3.5(0)
H2	0.026(4)	0.5555(24)	0.9029(24)	3.5(0)
H3	−0.070(4)	0.3770(25)	0.8678(25)	3.9(0)
H4	0.087(4)	0.2679(24)	0.8278(26)	3.6(0)
H5	0.355(4)	0.3203(23)	0.8349(24)	3.3(0)
H9	0.783(4)	0.8653(23)	0.8576(24)	2.9(0)
H10	0.681(4)	0.9638(23)	0.7484(23)	3.0(0)
H14	−0.162(4)	0.8348(24)	0.3396(24)	3.6(0)
H15	−0.409(4)	0.7633(24)	0.3492(25)	3.8(0)
H16	−0.434(4)	0.7434(25)	0.5075(26)	4.0(0)
H17	−0.215(4)	0.7924(25)	0.6574(25)	3.8(0)
H19A	0.613(4)	0.4290(24)	0.8738(25)	3.6(0)
H19B	0.715(4)	0.5409(25)	0.9127(25)	3.6(0)
H20A	0.524(4)	0.4503(29)	0.7048(29)	6.1(0)
H20B	0.638(5)	0.5571(28)	0.7455(31)	6.1(0)
H20C	0.708(4)	0.4616(30)	0.7395(31)	6.1(0)
H21A	0.280(4)	0.9828(25)	0.4746(26)	4.3(0)

(continued)

TABLE III. *(continued)*

Atom	*x*	*y*	*z*	B_{iso}
H21B	0.114(4)	0.9333(25)	0.3812(26)	4.3(0)
H22A	0.165(5)	0.7619(31)	0.3709(33)	7.5(0)
H22B	0.305(5)	0.8390(31)	0.3437(31)	7.5(0)
H22C	0.320(5)	0.8157(35)	0.4492(32)	7.5(0)
H23	0.240(5)	0.6453(31)	0.6949(30)	7.0(0)
H24A	0.036(5)	0.4177(30)	0.5412(31)	7.3(0)
H24B	0.089(5)	0.4971(31)	0.6604(31)	7.3(0)
H24C	0.198(5)	0.4180(32)	0.6288(33)	7.3(0)
H25A	0.315(5)	0.5549(33)	0.4538(35)	8.6(0)
H25B	0.178(5)	0.4579(35)	0.4199(35)	8.6(0)
H25C	0.350(5)	0.4588(35)	0.4947(38)	8.6(0)

TABLE IV. Selected Bond Distances (Å) and Angles (°) (e.s.d.s) for $[Cu_2(EtBITP)(OH)Cl_3]DMF$ (II)

Cu(1)–Cu(2)	3.017(1)	N(4)–C(13)	1.386(5)
Cu(1)–Cl(1)	2.2582(10)	N(4)–C(21)	1.458(5)
Cu(1)–Cl(3)	2.5643(10)	N(5)–N(6)	1.352(4)
Cu(1)–O(1)	1.9009(24)	N(5)–C(8)	1.318(4)
Cu(1)–N(1)	1.970(3)	N(6)–C(11)	1.316(4)
Cu(1)–N(5)	2.158(3)	C(8)–C(9)	1.389(5)
Cu(2)–Cl(2)	2.2607(10)	C(9)–C(10)	1.352(5)
Cu(2)–Cl(3)	2.5382(10)	C(10)–C(11)	1.390(5)
Cu(2)–O(1)	1.9111(25)	C(13)–C(14)	1.390(5)
Cu(2)–N(2)	1.978(3)	C(13)–C(18)	1.394(5)
Cu(2)–N(6)	2.130(3)	C(14)–C(15)	1.377(6)
S(1)–C(7)	1.748(3)	C(15)–C(16)	1.386(6)
S(1)–C(8)	1.766(3)	C(16)–C(17)	1.374(6)
S(2)–C(11)	1.762(3)	C(17)–C(18)	1.382(5)
S(2)–C(12)	1.752(4)	C(19)–C(20)	1.507(6)
N(1)–C(1)	1.396(4)	C(21)–C(22)	1.496(7)
N(1)–C(7)	1.318(4)	C(1)–C(2)	1.384(5)
N(2)–C(12)	1.320(4)	C(1)–C(6)	1.395(5)
N(2)–C(18)	1.395(4)	C(2)–C(3)	1.374(5)
N(3)–C(6)	1.382(4)	C(3)–C(4)	1.391(6)
N(3)–C(7)	1.359(4)	C(4)–C(5)	1.375(6)
N(3)–C(19)	1.462(5)	C(5)–C(6)	1.394(5)
N(4)–C(12)	1.362(4)		
Cl(1)–Cu(1)–Cl(3)	130.65(4)	Cl(2)–Cu(2)–N(2)	94.17(8)
Cl(1)–Cu(1)–O(1)	98.02(8)	Cl(2)–Cu(2)–N(6)	137.10(8)
Cl(1)–Cu(1)–N(1)	92.90(8)	Cl(3)–Cu(2)–O(1)	82.37(8)
Cl(1)–Cu(1)–N(5)	133.73(8)	Cl(3)–Cu(2)–N(2)	93.99(8)
Cl(3)–Cu(1)–O(1)	81.84(8)	Cl(3)–Cu(2)–N(6)	96.96(7)
Cl(3)–Cu(1)–N(1)	93.88(8)	O(1)–Cu(2)–N(2)	169.83(10)
Cl(3)–Cu(1)–N(5)	95.48(7)	O(1)–Cu(2)–N(6)	84.28(10)
O(1)–Cu(1)–N(1)	168.45(10)	N(2)–Cu(2)–N(6)	86.76(11)
O(1)–Cu(1)–N(5)	83.40(10)	Cu(1)–Cl(3)–Cu(2)	72.50(3)
N(1)–Cu(1)–N(5)	86.36(10)	C(7)–S(1)–C(8)	100.25(15)
Cl(2)–Cu(2)–Cl(3)	125.65(4)	C(11)–S(2)–C(12)	100.84(16)
Cl(2)–Cu(2)–O(1)	95.66(7)	Cu(1)–O(1)–Cu(2)	104.65(11)

$(PAP6Me)(OH)Cl_3]\cdot 3H_2O$ (Fig. 5) [2]. The copper–oxygen bridge bond lengths fall within the range 1.85–2.04 Å established for other related, hydroxo-bridged dicopper(II) complexes [1–3, 9–12]. The copper–nitrogen (diazine) bond lengths (Cu(1)–N(5) 2.158 Å; Cu(2)–N(6) 2.130 Å) are the longest observed so far, implying a somewhat weaker interaction to the diazine centre.

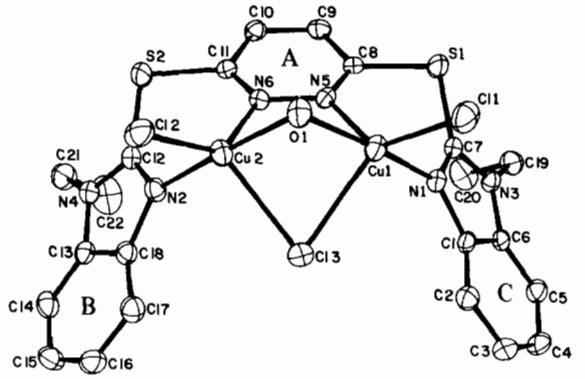

Fig. 4. Structural representation of $[Cu_2(EtBITP)(OH)Cl_3]\cdot$ DMF (**II**) with hydrogen atoms and DMF omitted (40% ellipsoids).

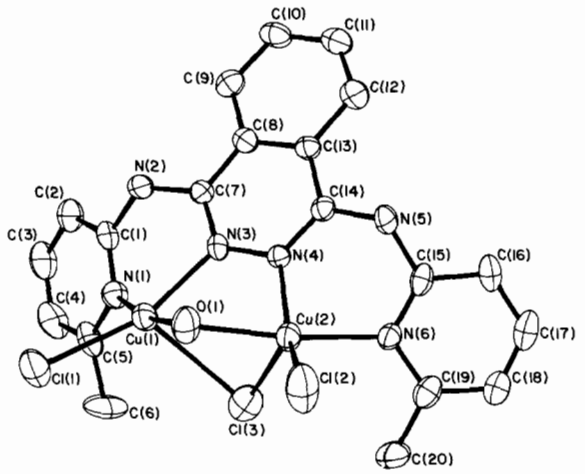

Fig. 5. Structural representation of $[Cu_2(PAP6Me)(OH)Cl_3]\cdot 3H_2O$ with hydrogen atoms and water omitted (40% ellipsoids).

The stereochemistry at each copper centre can best be described as a distorted trigonal-bipyramid. The axial ligands (N(1), O(1), N(2)) form an almost linear arrangement about the copper centres with angles N(1)–Cu(1)–O(1) and N(2)–Cu(2)–O(1) of 168.5° and 169.8° respectively. The largest equatorial angles are 133.7° and 137.1° (N(5)–Cu(1)–Cl(1) and N(6)–Cu(2)–Cl(2) respectively), and are much smaller than comparable angles in related compounds, e.g. $[Cu_2(PAP6Me)(OH)Cl_3]\cdot 3H_2O$ (149.4°, 158.4°) [2], $[Cu_2(PAP)(OH)Cl_3]\cdot 1.5H_2O$ (156.8°, 161.4°) [18] and $[Cu_2(PAP)(OH)(IO_3)_3]\cdot 4H_2O$ (153.4°, 154.0°) [9], which have been assigned distorted square-pyramidal geometries. Further support for this assignment comes from the very long copper–diazine nitrogen bond lengths, which would be associated with the minor orbital components of the d_{z^2} orbital. The ligand has a marked molecular fold, typical of hydroxo-bridged species of this sort, in order to accommodate the two five-coordinate metal centres. Such a fold is a result of the formation of six-membered chelate rings. For those complexes involving five-membered chelate rings the ligands adopt almost planar conformations (Fig. 2). The flat benzimidazole groups are mutually inclined by 91.4° and benzimidazoles B and C are inclined at angles of 47.2 and 49.9° respectively to the mean plane of the pyridazine ring (A) (Fig. 4).

Spectroscopy, Magnetism and Electrochemistry

The green, binuclear, hydroxo-bridged complexes are characterized in the infrared by absorptions in the range 3500–3620 cm^{-1} associated with hydroxide, O–H stretch. Other key infrared bands, together with their assignments, are listed in Table V. The visible absorption spectra of the binuclear copper(II) derivatives generally include a main band in the range 13 800–14 800 cm^{-1}, with a low energy shoulder. Spectral features of this sort have, in the past, been associated with five-coordinate copper(II). Typically, for a square-pyramidal copper(II) system, three features would be expected in the visible, while for a trigonal-bipyramidal system two should be observed, although, since distorted intermediate structures invariably prevail, such a distinction may not be possible [19]. In most cases complete resolution of the spectra of square-pyramidal systems is not possible at room temperature but at low temperature three transitions can be observed in some cases, e.g. for derivatives of the sort $[Cu_2(PAP)(RCOO)_3]$, which are assumed to have square-pyramidal stereochemistries [19]. The related complexes $[Cu_2(PAP)(OH)X_3]\cdot 1.5H_2O$ (X = Cl, Br), $[Cu_2(PAP)(OH)(IO_3)_3]\cdot 4H_2O$, which have distorted, intermediate five-coordinate structures, which are considered to be closer to a square-pyramid than a trigonal-bipyramid, exhibit broad, single absorptions in their solid state, mull transmittance spectra in the range 15 700–16 000 cm^{-1} with little resolution of this feature at low temperature [9, 18, 19]. Five-coordinate trigonal-bipyramidal copper(II) systems with similar ligands and chromophores would be expected to exhibit visible absorptions at significantly lower energies [19]. All of the binuclear, hydroxo-bridged complexes described in this study have visible absorptions below 15 000 cm^{-1} involving two resolved components at room temperature. These derivatives are therefore assumed to have five-coordinate structures similar to **II**, which has a distorted five-coordinate triply bridged structure in which the distortion is considered to lie closer to a trigonal-bipyramid.

The other copper(II) derivatives are mononuclear and appear to involve bidentate, rather than tetradentate ligands. The complex $[Cu(BuBITP)_2(H_2O)](ClO_4)_2\cdot 3H_2O$ (**XI**) exhibits higher energy visible absorption involving two well-resolved components. This compound is considered to be a five-coordinate derivative involving two in plane bidentate ligands

TABLE V. Infrared and Electronic Spectra and Magnetism

		Infrared (cm^{-1})	UV–Vis (cm^{-1})	μ_{eff} (BM) (RT)
I	$[Cu_2(MeBITP)(OH)Cl_3]\cdot H_2O$	3580(OH), 3480(H_2O)	14800, 11500(sh)	1.40
II	$[Cu_2(EtBITP)(OH)Cl_3]\cdot DMF$	3520(OH), 1660(DMF)	12050(191)[a]	1.38
III	$[Cu_2(EtBITP)(OH)Br_3]\cdot DMF$	3500(OH), 1650(DMF), 259, 243 (Cu–Br)	14300, 12500(sh)	1.34
IV	$[Cu(EtBITP)(NO_3)_2]\cdot H_2O$	3420(H_2O), 1745, 1734, 1718, 1700 (NO_3)	14900, 11500(sh)	1.84
V	$[Cu(EtBITP)]_2(ClO_4)_2\cdot 4H_2O$	3600(H_2O), 1090(ClO_4)		DIAM
VI	$[Cu_2(iPrBITP)(OH)Cl_3]\cdot 0.5H_2O$	3620(OH), 295, 275(Cu–Cl)	13800, 11900(sh)	1.68
VII	$[Cu_2(iPrBITP)(OH)Br_3]\cdot 0.5H_2O$	3620(OH), 240, 220(Cu–Br)	14300, 11800(sh)	1.45
VIII	$[Cu(iPrBITP)]_2(ClO_4)_2\cdot CH_3CN\cdot 2H_2O$	3500(H_2O), 1090(ClO_4)		DIAM
IX	$[Cu_2(BuBITP)(OH)Br_3]$	3590(OH), 236, 220(Cu–Br)	14700, 11600(sh)	1.44
X	$[Cu(BuBITP)(NO_3)_2]\cdot 1.5H_2O$	1734, 1720(sh) 1712(sh), 1700(NO_3)	16100, 11800(sh)	1.84
XI	$[Cu(BuBITP)_2(H_2O)](ClO_4)_2\cdot 3H_2O$	3400(H_2O), 1140, 1090(sh) 1070(ClO_4)	15900, 11400	2.02
XII	$[Cu(BuBITP)]_2(ClO_4)_2\cdot 0.2H_2O$	1085(ClO_4)		DIAM

[a]Solution in DMF, otherwise mull transmittance.

and an axial water similar to the square-pyramidal complex $[Cu(PTP)_2(H_2O)](ClO_4)_2\cdot 3H_2O$ which has been structurally characterized [4, 14]. The two nitrate complexes (**IV, X**) involve just one ligand per copper, clearly indicating nitrate coordination. The complexity of the nitrate combination band ($\nu_1 + \nu_4$) region in the infrared makes an assignment of the role of the nitrate groups difficult. However the presence of both monodentate and bidentate nitrates in each case is not unreasonable [20]. A square-pyramidal structure involving bidentate ligand and both mono- and bidentate nitrate is therefore assigned to these complexes. The 'normal' magnetic moments for these compounds are consistent with the assignment of these species as mononuclear copper(II) derivatives.

The diamagnetic copper(I) derivatives (**V, VIII, XII**) are red or orange in colour with no visible absorption in the range associated with copper(II) species. Perchlorate absorptions in the infrared are associated with ionic perchlorate groups and structurally all three derivatives are considered to be similar to the complex $[Cu_2(PTP)_2](ClO_4)_2$, which has been shown from X-ray crystallographic studies, to be a dimeric binuclear copper(I) complex involving two four-coordinate distorted tetrahedral copper(I) centres sandwiched between two tetradentate ligands [14].

Room temperature magnetic moments for the binuclear, hydroxo-bridged species lie in the range $\mu_{eff} = 1.34–1.68$ BM indicating antiferromagnetic exchange between the copper(II) centres. The lower values associated with the bromo-derivatives for the pairs of compounds **II, III** and **VI, VII** suggests that a bridging bromine atom is likely to be present in these compounds. It is well established that for structurally similar halogen bridged dicopper(II) species antiferromagnetic exchange is stronger for bromo-bridged compounds [21]. The larger difference in the case of the ligand iPrBITP may indicate a structural anomaly involving differences in the hydroxide bridge angle, since the hydroxide bridge will undoubtedly dominate the exchange situation.

A variable temperature magnetic study was carried out on $[Cu_2(EtBITP)(OH)Cl_3]\cdot DMF$ in the range 5–300 K. The results are summarized in Fig. 6. The

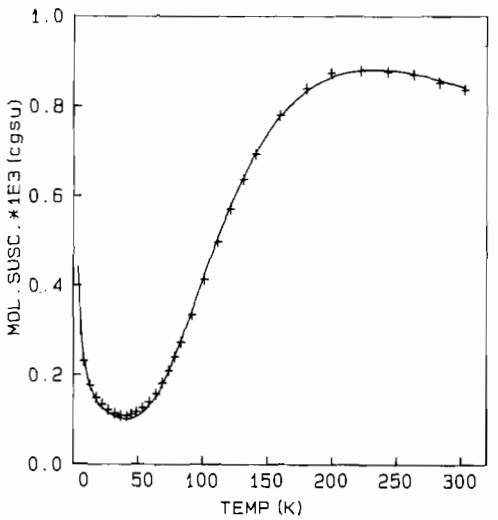

Fig. 6. Magnetic susceptibility data for $[Cu_2(EtBITP)(OH)Cl_3]\cdot DMF$ (II). The solid line was calculated from eqn. (1) with $g = 2.01 \pm 0.01$, $-2J = 260 \pm 1$ cm^{-1} and $N\alpha = 60 \times 10^{-6}$ cgs units (cm^3 mol^{-1})/Cu and assuming 0.4% paramagnetic impurity ($\rho = 0.004$).

best fit line was calculated from the Van Vleck equation [22] for exchange-coupled pairs of copper(II) ions (eqn. (1))

$$\chi_M = \frac{N\beta^2 g^2}{3kT}\left[1 + \tfrac{1}{3}\{\exp(-2J/kT)\}\right]^{-1}(1-\rho) + \left[\frac{N\beta^2 g^2}{4kT}\right]\rho + N\alpha \quad (1)$$

In this expression $2J$ (in the spin Hamiltonian $\mathcal{H} = 2J\hat{s}_1\cdot\hat{s}_2$) is the singlet–triplet splitting or exchange integral and other symbols have their usual meaning. ρ represents the fraction of a possible magnetically dilute impurity. The temperature independent paramagnetism, $N\alpha$, was taken as 120×10^{-6} cgs units/mol. The parameters giving the best fit were obtained by using a non-linear regression analysis with ρ as a floating parameter. The exchange integral for **II** ($-2J = 260$ cm^{-1}) indicates moderate exchange between the copper(II) centres. Comparable exchange would therefore be expected for compounds **I**, **III**, **VII** and **IX**.

The copper stereochemistry in **II** is considered to be approximately trigonal-bipyramidal, which would involve a d_{z^2} copper ion ground state. The major lobes of the magnetic orbital would therefore point towards the bridging oxygen atom and so equatorial magnetic interactions to the pyridazine bridge would be considered to be relatively small. In previous examples of square-pyramidal hydroxo-bridged copper(II) complexes of tetradentate phthalazine and pyridazine ligands significant copper–diazine nitrogen magnetic interactions occur via in plane $d_{x^2-y^2}$ orbital overlap [1, 3, 9–12, 19]. Also for related, square-pyramidal phthalazine complexes involving in plane magnetic interactions to both hydroxide and diazine bridge groups, an almost linear relationship was found to exist between hydroxide bridge angle and exchange [9–12]. The relationship $-2J = 24.27\,\phi - 2274$ cm^{-1} was found for six complexes with ϕ(Cu–O(H)–Cu bridge angle) in the range 100–126°. A general comparison of square-pyramidal, hydroxide bridged complexes of phthalazine and pyridazine ligands, involving $d_{x^2-y^2}$ diazine magnetic interactions, also reveals that significantly larger exchange integrals occur for pyridazine systems [3]. With this in mind it is of interest to note that compound **II** unexpectedly conforms to the above linear relationship, based on bridge angle (for ϕ = 104.7° $-2J_{calc} = 267$ cm^{-1}). This suggests that while in the previous examples a significant, but approximately constant, contribution to total exchange arises from the phthalazine bridge, for **II** the pyridazine contribution must be smaller than that expected for a $d_{x^2-y^2}$ system, thus supporting the assignment of a trigonal-bipyramidal stereochemistry.

Electrochemical studies have been carried out on a number of the binuclear complexes and the results are reported in Table VI. Cyclic voltammetry in DMF using a glassy carbon electrode gave single redox waves for each compound with $E_{1/2}$ in the range 0.41–0.46 V (*versus* SCE). Figure 7 shows cyclic voltammograms at varying scan rates for [Cu_2(EtBITP)(OH)Cl_3]·DMF in DMF. ΔE_p varies slightly as a function of scan rate (100 mV at 25 mV s^{-1} to 120 mV at 200 mV s^{-1}) indicating a quasi-reversible redox process. Identical cyclic voltammograms are obtained by scanning in a positive voltage direction (Fig. 7a) and by scanning in a negative voltage direction (Fig. 7b) confirming the unique nature of the redox process. No other electrochemical feature is observed for this complex in the range 0.8 to −1.2 V (Fig. 8). The ligands also do not display any electrochemical activity in this voltage range. For the other compounds similar electrochemistry is observed, but, with the exception of **I**, ΔE_p is generally much larger and varies significantly as a function of scan rate indicating non-reversible redox processes. The single redox wave is associated with two electron reduction in DMF in each case and this is supported by coulometric measurements.

Somewhat reduced coulomb counts are observed for these complexes on reduction in DMF at +0.1 V,

TABLE VI. Electrochemical Data

		$E_{1/2}$ (V (*vs.* SCE))	ΔE_p (mV)[a]
I	[Cu_2(MeBITP)(OH)Cl_3]·H_2O	0.45[b]	120[q]
II	[Cu_2(EtBITP)(OH)Cl_3]·DMF	0.43[b]	120[q]
III	[Cu_2(EtBITP)(OH)Br_3]·DMF	0.41[b]	260[n]
VI	[Cu_2(iPrBITP)(OH)Cl_3]·0.5H_2O	0.43[b]	150[n]
VII	[Cu_2(iPrBITP)(OH)Br_3]·0.5H_2O	0.46[b]	180[n]
IX	[Cu_2(BuBITP)(OH)Br_3]	0.42[c]	260[n]
		0.42[b]	240[n]

[a]Peak to peak separation at scan rate of 200 mV s^{-1}. [b]Glassy carbon/DMF/TEAP/SCE. [c]Platinum/DMF/TEAP/SCE. [q]Quasi-reversible. [n]Non-reversible.

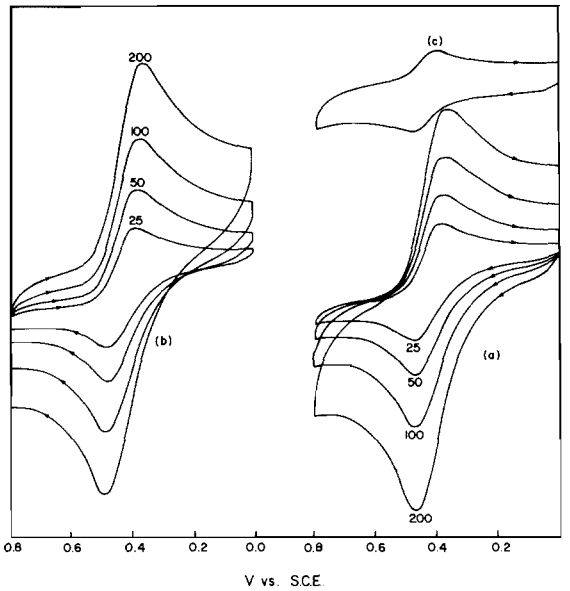

Fig. 7. (a) Cyclic voltammograms for $[Cu_2(EtBITP)(OH)Cl_3]\cdot DMF$ in DMF (1×10^{-3} M, 0.1 M TEAP, G.C., SCE). Scan rate 25–200 mV s^{-1} at positive scan from 0.0–0.8 V. (b) Negative scan from 0.8–0.0 V. (c) Ferrocene/ferrocinium couple.

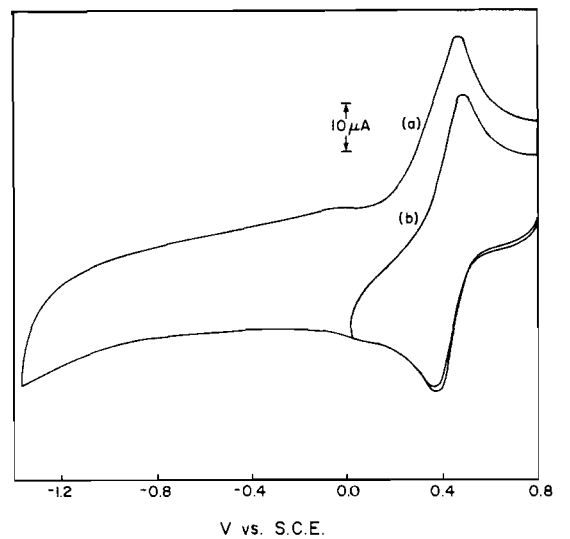

Fig. 8. (a) Cyclic voltammogram for $[Cu_2(EtBITP)(OH)Cl_3]\cdot DMF$ (II) in DMF (1×10^{-3} M, 0.1 M TEAP, G.C., SCE) scanned at 200 mV s^{-1} from 0.8 to −1.4 V. (b) Same as Fig. 7b.

indicating that a spontaneous redox process has occurred in these solvents. This phenomenon has been observed with other binuclear copper(II) complexes with high redox potentials, both in DMF and acetonitrile [4, 12]. If, however, the DMF solutions of the binuclear copper(II) complexes are first fully oxidized at +0.8 V and then reduced at +0.1 V the coulomb counts are very close two electron equivalents. The same observation can be made by examining the visible absorption spectrum of systems of this sort in DMF. For example a DMF solution of $[Cu_2(EtBITP)(OH)Cl_3]\cdot DMF$ (II) (1×10^{-3} M), made by stirring the solid/solvent mixture overnight, gave a visible absorption at 12 050 cm^{-1} with molar absorbance of 124 l mol^{-1} cm^{-1}. If this solution is oxidized at +0.8 V, fully reduced at +0.1 V (two electron equivalents of charge required) and then fully oxidized at +0.8 V, the same absorption maximum is observed (Fig. 9) but the extinction coefficient is increased (E = 191 l mol^{-1} cm^{-1}).

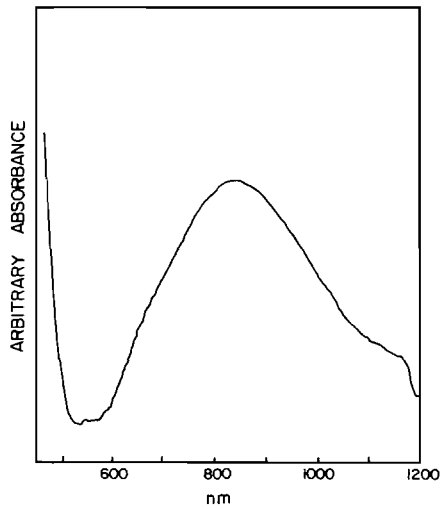

Fig. 9. Visible absorption spectrum (DMF) for $[Cu_2(EtBITP)(OH)Cl_3]\cdot DMF$ (II) after electrochemical oxidation at +0.8 V.

Supplementary Material

Anisotropic thermal parameters and a listing of structure factors for all compounds are available from the authors on request.

Acknowledgements

We thank the Natural Sciences and Engineering Research Council of Canada for financial support for this study, including the purchase of the Faraday Susceptometer, and Dr. M. J. Newlands for graphics assistance.

References

1 L. K. Thompson, T. C. Woon, D. B. Murphy, E. J. Gabe, F. L. Lee and Y. LePage, *Inorg. Chem.*, *24*, 4719 (1985).
2 S. K. Mandal, L. K. Thompson and A. W. Hanson, *J. Chem. Soc., Chem. Commun.*, 1709 (1985).
3 L. K. Thompson, S. K. Mandal, E. J. Gabe, F. L. Lee and A. W. Addison, *Inorg. Chem.*, *26*, 657 (1987).

4 T. C. Woon, R. McDonald, S. K. Mandal, L. K. Thompson, S. P. Connors and A. W. Addison, *J. Chem. Soc., Dalton Trans.*, 2381 (1986).
5 M. Ghedini, G. DeMunno, G. Denti, A. M. Manotti Lanfredi and A. Tiripicchio, *Inorg. Chim. Acta, 57,* 87 (1982).
6 P. Dapporto, G. DeMunno, G. Bruno and M. Romeo, *Acta Crystallogr., Sect. C, 39,* 718 (1983).
7 G. DeMunno and G. Denti, *Acta Crystallogr., Sect. C, 40,* 616 (1984).
8 P. Dapporto, G. DeMunno, A. Sega and C. Mealli, *Inorg. Chim. Acta, 83,* 171 (1984).
9 L. K. Thompson, *Can. J. Chem., 61,* 579 (1983).
10 L. K. Thompson, F. W. Hartstock, P. Robichaud and A. W. Hanson, *Can. J. Chem., 62,* 2755 (1984).
11 L. K. Thompson, A. W. Hanson and B. S. Ramaswamy, *Inorg. Chem., 23,* 2459 (1984).
12 S. K. Mandal, T. C. Woon, L. K. Thompson, M. J. Newlands and E. J. Gabe, *Aust. J. Chem., 39,* 1007 (1986).
13 L. K. Thompson, unpublished results.
14 S. K. Mandal, L. K. Thompson, E. J. Gabe, F. L. Lee and J. P. Charland, *Inorg. Chem.*, in press.
15 G. Germain, P. Main and M. M. Woolfson, *Acta Crystallogr., Sect. A, 27,* 368 (1971).
16 E. J. Gabe, F. L. Lee and Y. LePage, in G. Sheldrick, C. Kruger and R. Goddard (eds.), 'Crystallographic Computing III, Clarendon, Oxford, 1985, p. 167.
17 'International Tables for X-ray Crystallography, Vol. IV, Kynoch Press, Birmingham, U.K., 1974, Table 2.2B, p. 99.
18 G. Marongiu and E. C. Lingafelter, *Acta Crystallogr., Sect. B, 38,* 620 (1982).
19 L. K. Thompson, V. T. Chacko, J. A. Elvidge, A. B. P. Lever and R. V. Parish, *Can. J. Chem., 47,* 4141 (1969).
20 A. B. P. Lever, E. Mantovani and B. S. Ramaswamy, *Can. J. Chem., 49,* 1957 (1971).
21 R. D. Willett, *Inorg. Chem., 25,* 1918 (1986).
22 J. H. Van Vleck, 'The Theory of Electric and Magnetic Susceptibilities, Oxford University Press, London, 1932, Chap. 9.